

## Supplementary Information

### 2-Aza-1,3-butadiene ligands for the selective detection of Hg<sup>2+</sup> and Cu<sup>2+</sup> ions

Rosario Martínez, Fabiola Zapata, Antonio Caballero, Arturo Espinosa, Alberto Tárraga\*, and Pedro Molina\*

*Departamento de Química Orgánica. Facultad de Química. Universidad de Murcia. Campus de Espinardo, 30071 Murcia. Spain*

*E-mail: [atarraga@um.es](mailto:atarraga@um.es); [pmolina@um.es](mailto:pmolina@um.es)*

**Dedicated to Professor Benito Alcaide on the occasion of his 60<sup>th</sup> anniversary**

#### Contents

<b>Figure SI 1:</b> Cyclic voltammogram of <b>7</b>	S3
<b>Figure SI 2:</b> Cyclic voltammogram of <b>9</b>	S3
<b>Figure SI 3:</b> Changes in the linear sweep voltammogram of <b>7</b> upon addition of increasing amounts of Cu <sup>2+</sup> cations and Hg <sup>2+</sup> cations.	S4
<b>Figure SI 4:</b> Changes in the linear sweep voltammogram of <b>9</b> upon addition of increasing amounts of Cu <sup>2+</sup> cations and Hg <sup>2+</sup> cations.	S4
<b>Figure SI 5:</b> Evolution of the DPV of <b>6</b> upon addition of increasing amounts of Zn <sup>2+</sup> cations.	S5
<b>Figure SI 6:</b> Changes in the absorption spectra of <b>6</b> and <b>7</b> in CH <sub>3</sub> CN upon addition of increasing amounts of Hg <sup>2+</sup> .	S5
<b>Figure SI 7:</b> Fluorescence emission spectra of ligands <b>6</b> and <b>8</b> in CH <sub>3</sub> CN upon titration with Hg <sup>2+</sup> .	S6
<b>Figure SI 8:</b> Evolution of the fluorescence emission spectra of <b>8</b> in CH <sub>3</sub> CN upon addition of increasing amounts of Zn <sup>2+</sup>	S6
<b>Figure SI 9:</b> Evolution of the UV/visible spectra of <b>10</b> in CH <sub>3</sub> CN upon addition of increasing amounts of Cu <sup>2+</sup> and Hg <sup>2+</sup>	S7
<b>Figure SI 10:</b> Evolution of the fluorescence emission spectra of <b>10</b> in CH <sub>3</sub> CN upon addition of increasing amounts of Cu <sup>2+</sup> and Hg <sup>2+</sup>	S7
<b>Figure SI 11:</b> Job's plot for <b>7</b> and <b>9</b> with Hg <sup>2+</sup>	S8
<b>Figure SI 12:</b> Job's plot for <b>10</b> and Cu <sup>2+</sup>	S8
<b>Figure SI 13:</b> Stepwise complexation/descomplexation cycles of ligands <b>7</b> and <b>9</b> with Hg <sup>2+</sup>	S9
<b>Figure SI 14:</b> Stepwise complexation/descomplexation cycles of	

ligand <b>10</b> and $\text{Cu}^{2+}$	S9
<b>Figure SI 15.</b> Plot for determining the detection limit of <b>6</b> towards $\text{Hg}^{2+}$	S10
<b>Figure SI 16.</b> Plot for determining the detection limit of <b>7</b> towards $\text{Hg}^{2+}$	S10
<b>Figure SI 17.</b> Plot for determining the detection limit of <b>8</b> towards $\text{Hg}^{2+}$	S11
<b>Figure SI 18.</b> Plot for determining the detection limit of <b>8</b> towards $\text{Zn}^{2+}$	S11
<b>Figure SI 19.</b> Plot for determining the detection limit of <b>9</b> towards $\text{Hg}^{2+}$	S12
<b>Figure SI 20.</b> Plot for determining the detection limit of <b>10</b> towards $\text{Hg}^{2+}$	S12
<b>Figure SI 21.</b> Plot for determining the detection limit of <b>10</b> towards $\text{Cu}^{2+}$	S13
<b>Calculated structures:</b> cartesian coordinates and energies	S14

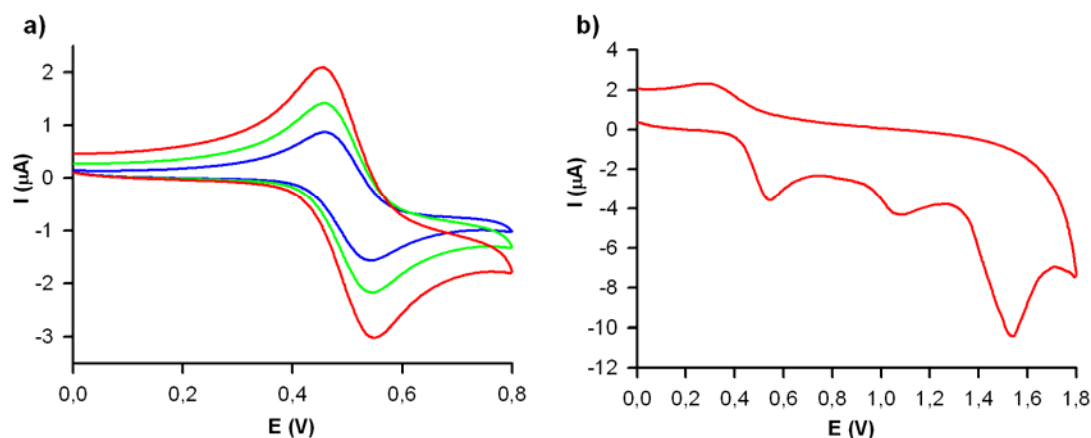


**Figure SI 1:** Cyclic voltammogram of **7** in CH<sub>3</sub>CN using n-Bu<sub>4</sub>NPF<sub>6</sub> 0,1 M as the supporting electrolyte, AgCl/Ag as the reference electrode, and platinum wires as the counter and working electrodes, in the presence of DMFc as the internal standard. a) Different scanning rates were used to check the reversibility of the system: (blue) 0.10 V s<sup>-1</sup>, (green) 0.30 V s<sup>-1</sup>, (red) 0.50 V s<sup>-1</sup>. b) 0.50 V s<sup>-1</sup>.

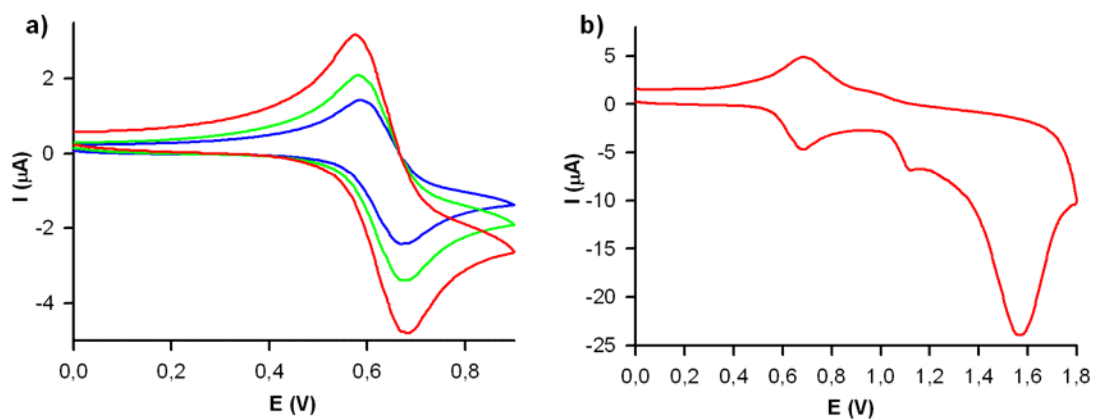


**Figure SI 2:** Cyclic voltammogram of **9** in CH<sub>3</sub>CN using n-Bu<sub>4</sub>NPF<sub>6</sub> 0,1 M as the supporting electrolyte, AgCl/Ag as the reference electrode, and platinum wires as the counter and working electrodes, in the presence of DMFc as the internal standard. a) Different scanning rates were used to check the reversibility of the system: (blue) 0.10 V s<sup>-1</sup>, (green) 0.30 V s<sup>-1</sup>, (red) 0.50 V s<sup>-1</sup>. b) 0.50 V s<sup>-1</sup>.

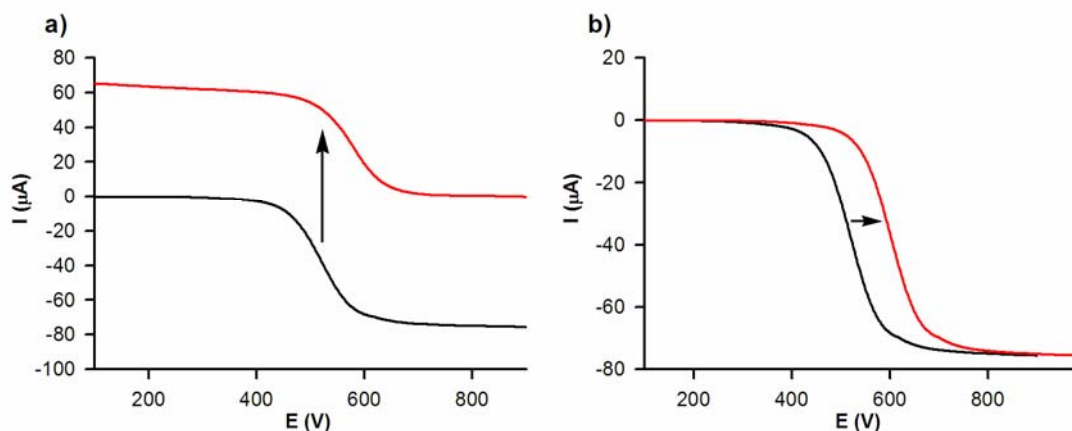


**Figure SI 3:** Changes in the linear sweep voltammogram of **7** ( $1 \times 10^{-3}$  M) in  $\text{CH}_3\text{CN}$  with TBAP (0.1 M) as supporting electrolyte, obtained using a rotating disk electrode at  $100 \text{ mV s}^{-1}$  and 1000 rpm, when metal cations are added: (a) upon addition of increasing amounts of  $\text{Cu}^{2+}$  cations and (b) upon addition of increasing amount of  $\text{Hg}^{2+}$  cations.

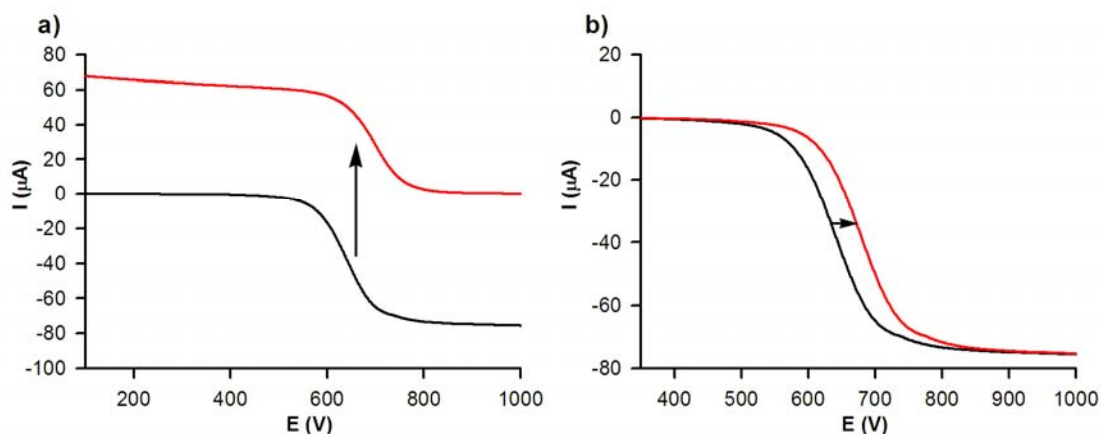


**Figure SI 4:** Changes in the linear sweep voltammogram of **9** ( $1 \times 10^{-3}$  M) in  $\text{CH}_3\text{CN}$  with TBAP (0.1 M) as supporting electrolyte, obtained using a rotating disk electrode at  $100 \text{ mV s}^{-1}$  and 1000 rpm, when metal cations are added: (a) upon addition of increasing amounts of  $\text{Cu}^{2+}$  cations and (b) upon addition of increasing amount of  $\text{Hg}^{2+}$  cations.

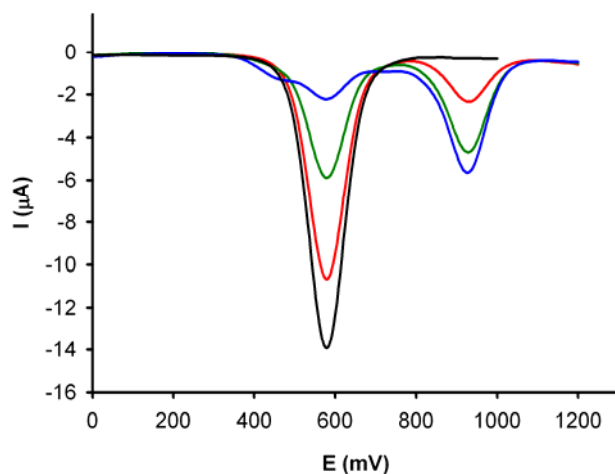


**Figure SI 5:** Evolution of the DPV of **6** ( $1 \times 10^{-3}$  M) in  $\text{CH}_3\text{CN}$  with TBAP (0.1 M) as supporting electrolyte scanned at  $0.1 \text{ V}\cdot\text{s}^{-1}$  from -0 to 1.2 V when  $\text{Hg}(\text{ClO}_4)_2$  is added: from 0 (black line) to 1 equiv (blue line).

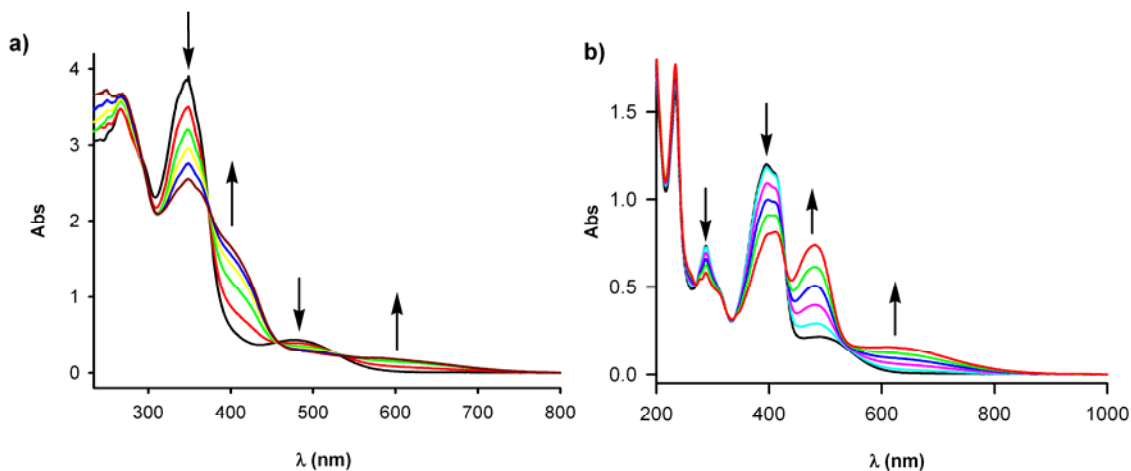


**Figure SI 6:** Changes in the absorption spectra of **6** a) and **7** b) ( $1 \times 10^{-4}$  M) in  $\text{CH}_3\text{CN}$  upon addition of increasing amounts of  $\text{Hg}^{2+}$  ( $2.5 \times 10^{-2}$  M) in  $\text{CH}_3\text{CN}$ . Arrows indicate the absorption that increase or decrease during the experiment.

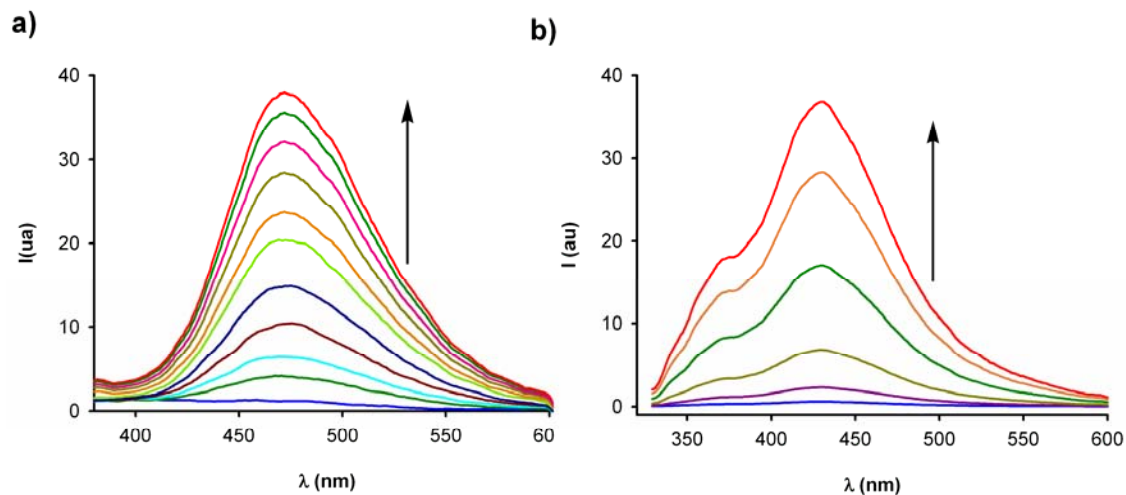


**Figure SI 7:** Fluorescence emission spectra of ligands **6** (a) and **8** (b) in CH<sub>3</sub>CN ( $c = 2.5 \times 10^{-5}$  M,  $\lambda_{\text{exc}} = 310$  nm) upon titration with Hg<sup>2+</sup>. The initial spectra (blue) correspond to the free ligands **6** or **8** and the final spectra (red) correspond to the complexed forms **6**·Hg<sup>2+</sup> and **8**·Hg<sup>2+</sup> after addition of 1 equiv of Hg<sup>2+</sup>.

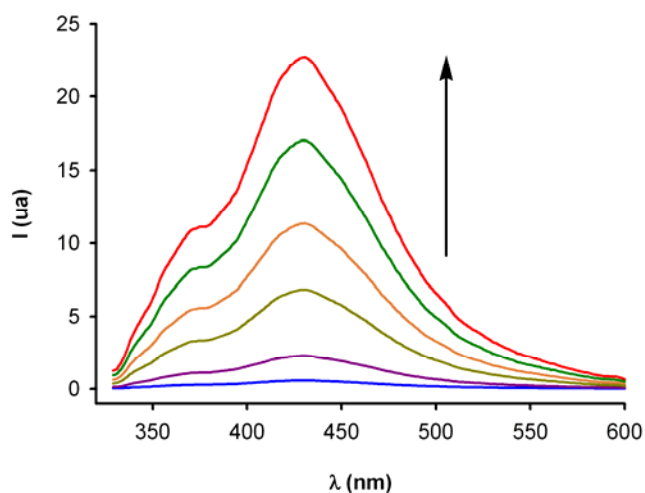


**Figure SI 8:** Fluorescence emission spectra of ligand **8** in CH<sub>3</sub>CN ( $c = 2.5 \times 10^{-5}$  M,  $\lambda_{\text{exc}} = 310$  nm) upon titration with Zn<sup>2+</sup>. The initial spectra (blue) correspond to the free ligand **8** and the final spectra (red) correspond to the complexed form **8**·Zn<sup>2+</sup>.

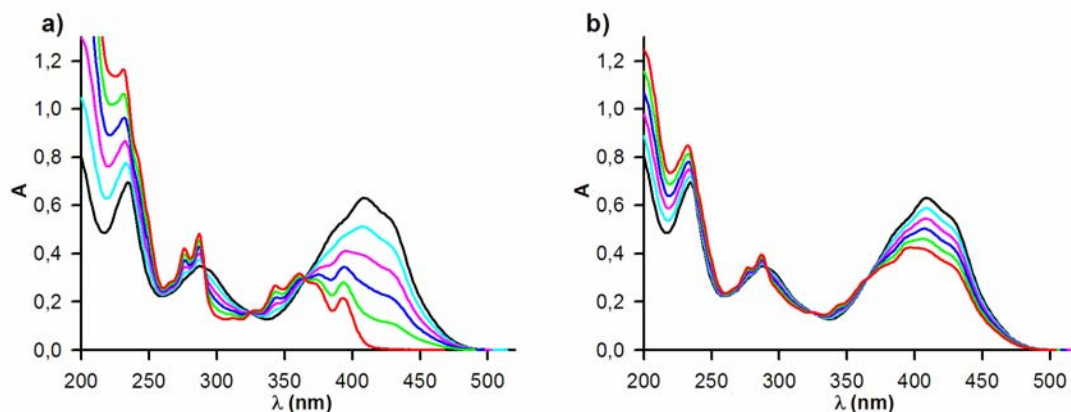


**Figure SI 9:** UV/visible spectra obtained during the titration of **10** in  $\text{CH}_3\text{CN}$  ( $c = 2.5 \times 10^{-5}$  M) with  $\text{Cu}^{2+}$  (a) and  $\text{Hg}^{2+}$  (b). The initial spectra (black) correspond to the free ligand **10** and the final spectra (red) correspond to the complexed forms  $\mathbf{10} \cdot \text{Cu}^{2+}$  and  $\mathbf{10} \cdot \text{Hg}^{2+}$  after addition of 1 equiv of  $\text{Cu}^{2+}$  or  $\text{Hg}^{2+}$  respectively.

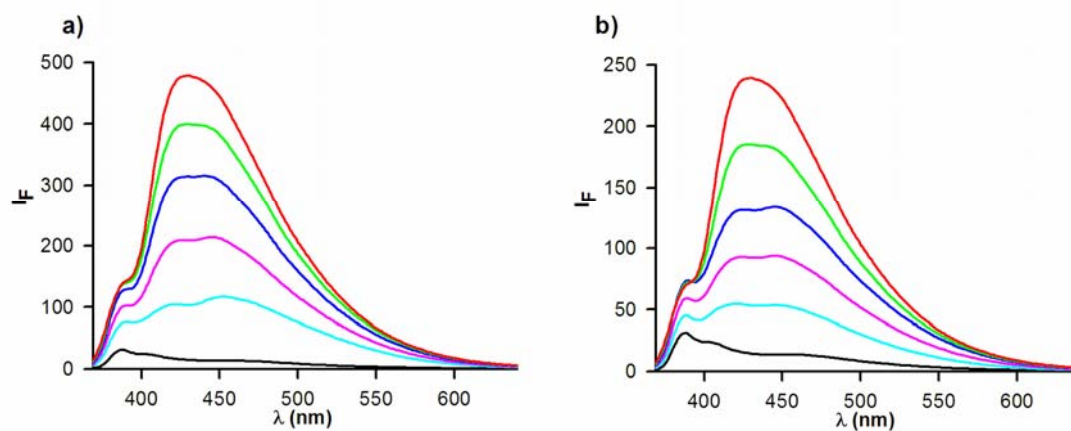


**Figure SI 10:** Fluorescence emission spectra obtained during the titration of **10** in  $\text{CH}_3\text{CN}$  ( $c = 2.5 \times 10^{-5}$  M,  $\lambda_{\text{exc}} = 350$  nm) with  $\text{Cu}^{2+}$  (a) and  $\text{Hg}^{2+}$  (b). The initial spectra (black) correspond to the free ligand **10** and the final spectra (red) correspond to the complexed forms  $\mathbf{10} \cdot \text{Cu}^{2+}$  and  $\mathbf{10} \cdot \text{Hg}^{2+}$  after addition of 1 equiv of  $\text{Cu}^{2+}$  or  $\text{Hg}^{2+}$  respectively.

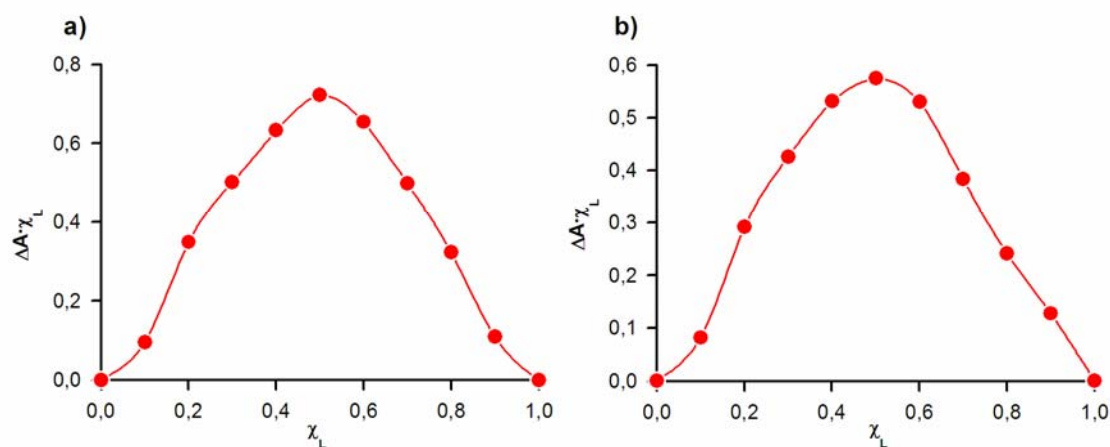


**Figure SI 11:** Job's plot for **7** (a) and **9** (b) titrated with  $\text{Hg}^{2+}$  indicating the formation of 1:1 complexes. The total  $[\text{L}] + [\text{Hg}^{2+}] = 1 \times 10^{-4} \text{ M}$ , illustrating the 1:1 stoichiometry of the complexed formed

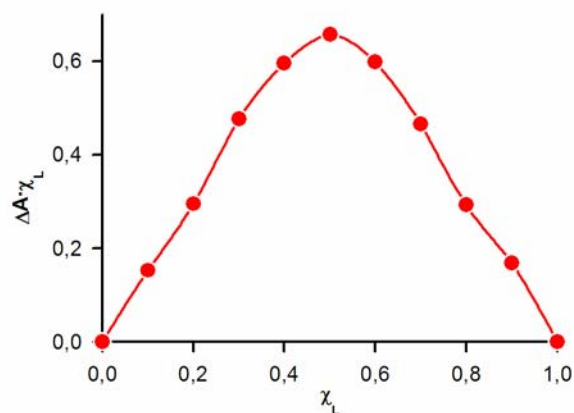


**Figure SI 12:** Job's plot for **10** and  $\text{Cu}^{2+}$  indicating the formation of 1:1 complexes. The total  $[\text{10}] + [\text{Cu}^{2+}] = 1 \times 10^{-4} \text{ M}$ , illustrating the 1:1 stoichiometry of the complexed formed.



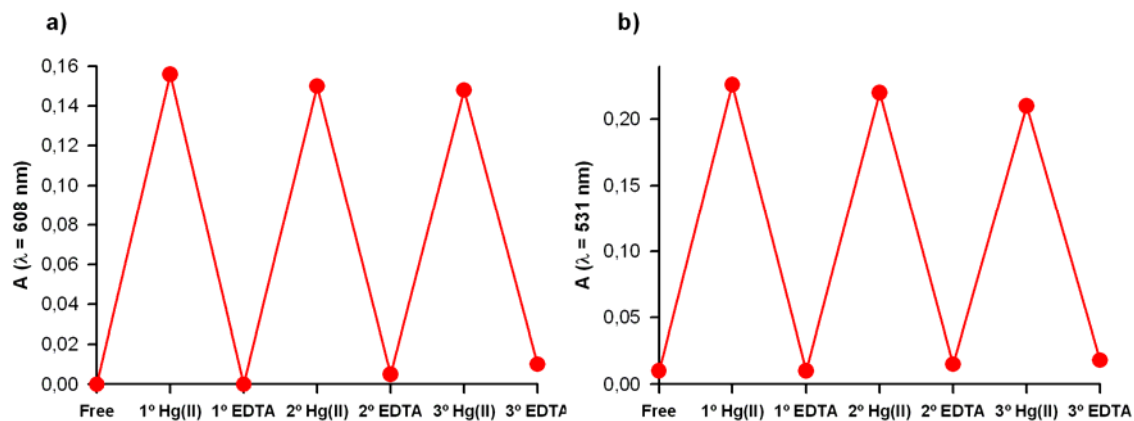


**Figure SI 13:** Stepwise complexation/descomplexation cycles of ligands **7** (a) and **9** (b) ( $2.5 \cdot 10^{-5}$  M in  $\text{CH}_3\text{CN}$ ) and  $\text{Cu}^{2+}$ , using EDTA as descomplexation agent; carried out by UV-Vis analysis.

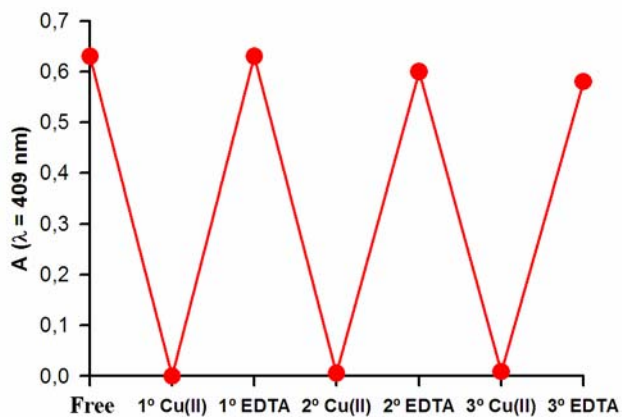


**Figure SI 14:** Stepwise complexation/descomplexation cycles of ligand **10** ( $2.5 \cdot 10^{-5}$  M in  $\text{CH}_3\text{CN}$ ) and  $\text{Cu}^{2+}$ , using EDTA as descomplexation agent; carried out by UV-Vis analysis.

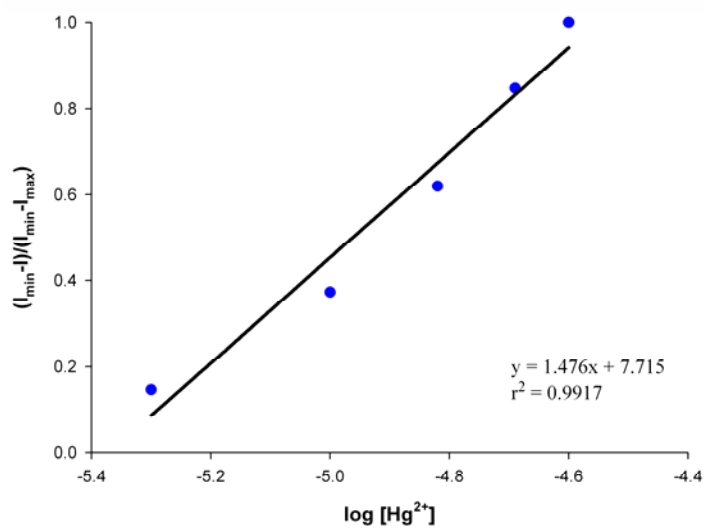


**Figure SI 15.** Plot for determining the detection limit of **6** towards Hg<sup>2+</sup>.

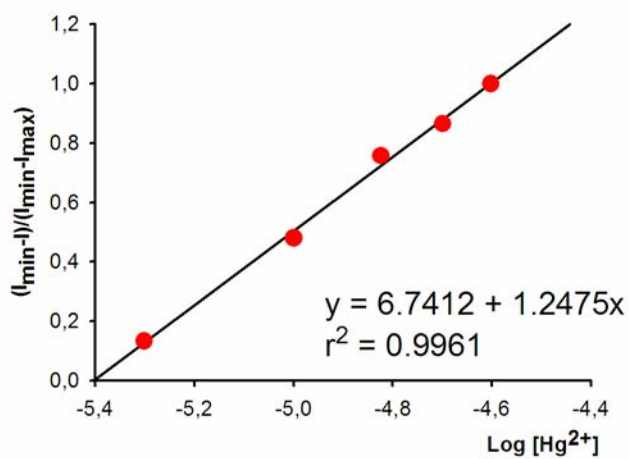


**Figure SI 16.** Plot for determining the detection limit of **7** towards Hg<sup>2+</sup>.

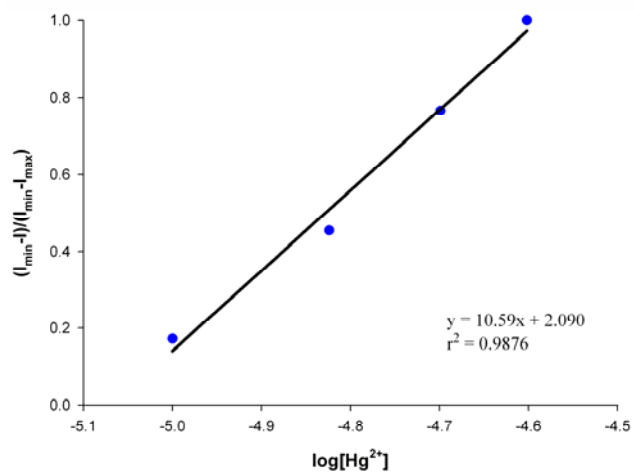


**Figure SI 17.** Plot for determining the detection limit of **8** towards  $\text{Hg}^{2+}$ .

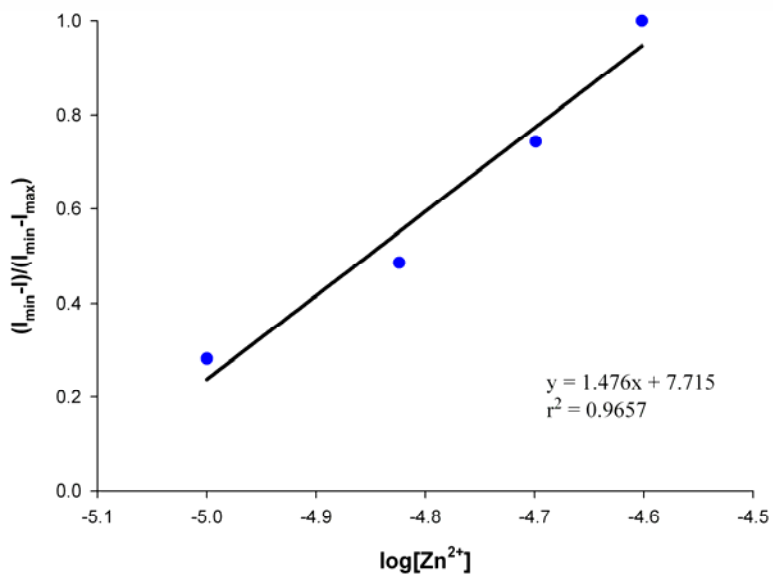


**Figure SI 18.** Plot for determining the detection limit of **8** towards  $\text{Zn}^{2+}$ .

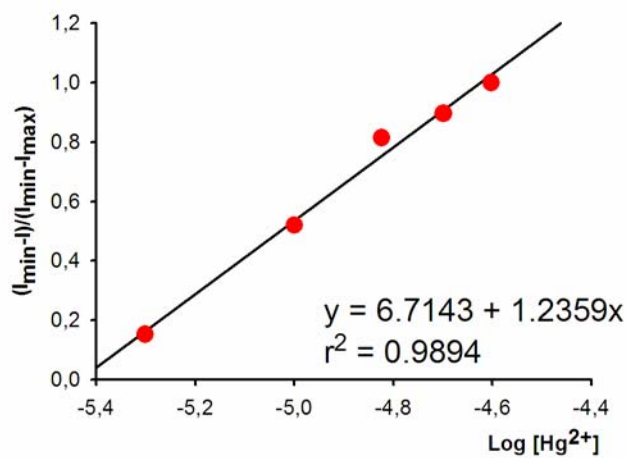


**Figure SI 19.** Plot for determining the detection limit of **9** towards Hg<sup>2+</sup>.

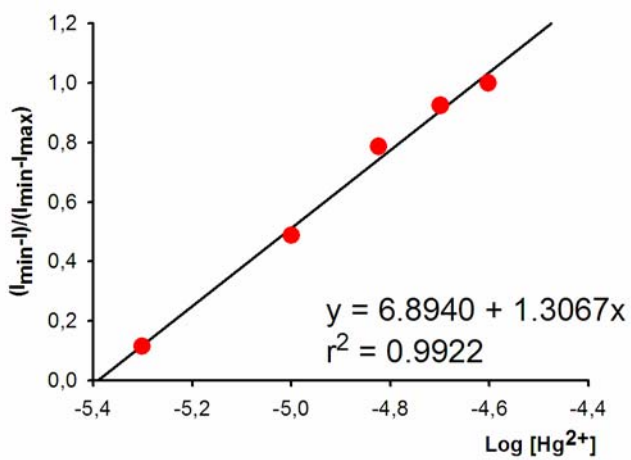


**Figure SI 20.** Plot for determining the detection limit of **10** towards Hg<sup>2+</sup>.

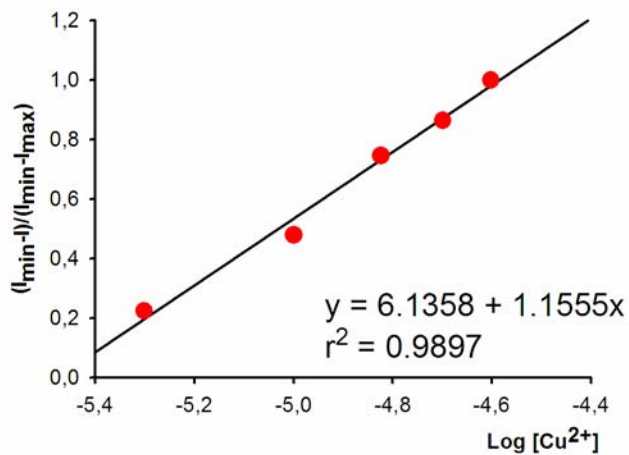


**Figure SI 21.** Plot for determining the detection limit of **10** towards Cu<sup>2+</sup>.

**Calculated structures:** cartesian coordinates (in Å) and energies (au) computed for Hg(OTf)<sub>2</sub>, compound **6** and complex **6**·Hg(OTf)<sub>2</sub>.-

**Hg(OTf)<sub>2</sub> (C<sub>i</sub>):**  $E_{\text{MeCN}} = -2076.368870$  au  
 $E_{\text{gas-phase}} = -2076.353567$  au

Hg	0.00000000	0.00000000	0.00000000
O	2.12336930	0.00000000	0.00000000
S	2.57798908	1.52826093	0.00000000
O	3.61124187	1.80477361	0.99035298
O	1.33621710	2.35048323	-0.08311408
C	3.39468823	1.62643249	-1.72124526
F	2.48998017	1.26891567	-2.65252958
F	3.79281088	2.88428995	-1.94444294
F	4.44442770	0.80064508	-1.77610467
O	-3.61124186	-1.80477361	-0.99035298
S	-2.57798908	-1.52826093	0.00000000
O	-2.12336930	-0.00000000	0.00000000
O	-1.33621709	-2.35048324	0.08311408
C	-3.39468823	-1.62643249	1.72124526
F	-3.79281088	-2.88428995	1.94444294
F	-2.48998017	-1.26891567	2.65252958
F	-4.44442770	-0.80064509	1.77610467

**Compound 6:**  $E_{\text{MeCN}} = -2206.548381$  au  
 $E_{\text{gas-phase}} = -2206.551698$  au

C	0.00000000	0.00000000	0.00000000
N	1.29812265	0.00000000	0.00000000
C	1.95150150	1.21243241	0.00000000
C	3.30980271	1.28160877	0.00729567
H	-0.56680079	0.95253203	-0.00216619
H	1.34627761	2.13456360	0.00225608
H	3.85565129	0.33567389	0.03387862
C	-0.79760149	-1.21876295	0.00306461
C	-2.22009691	-1.11690437	0.00430153
C	-3.01106638	-2.24245882	0.00733623
C	-2.43265756	-3.54106904	0.00897543
C	-3.21630793	-4.72369392	0.01189239
C	-2.61895808	-5.96838884	0.01321114
C	-1.20681999	-6.08452103	0.01188949
C	-0.41575010	-4.95539528	0.00927346
C	-0.99763281	-3.65619133	0.00766162
C	-0.21138405	-2.48257652	0.00481083
H	-2.67593841	-0.12470351	0.00328664
H	-4.09886369	-2.15303590	0.00857150
H	-4.30402281	-4.63223298	0.01303555
H	-3.23353681	-6.86901454	0.01545446
H	-0.74794955	-7.07356936	0.01317830
H	0.67224845	-5.03944611	0.00863361
H	0.87721481	-2.55393323	0.00431020
C	4.09145769	2.49846567	0.00569071
C	5.52015258	2.56506605	0.21732045
C	5.93185220	3.93069741	0.13181230

C	4.77415727	4.72422704	-0.15506386
C	3.64612835	3.84969870	-0.24686737
H	6.16351499	1.71107258	0.41057168
H	6.94849069	4.29860084	0.23471334
H	4.76062371	5.79894673	-0.31164009
H	2.62985442	4.14925060	-0.48512989
Fe	5.06082244	3.32536365	-1.60645489
C	5.23749544	1.94396513	-3.09952990
C	4.16336843	2.85177631	-3.37399509
C	4.70715212	4.17648336	-3.42527395
C	6.11584154	4.08670866	-3.18018742
C	6.44312675	2.70688760	-2.97782818
H	5.14448911	0.86958459	-2.97155823
H	3.11772463	2.58334139	-3.49172864
H	4.14582555	5.09130984	-3.59082486
H	6.80866409	4.92127772	-3.12632899
H	7.42743575	2.31229702	-2.74387540

Complex **6**-Hg(OTf)<sub>2</sub> :             $E_{\text{MeCN}} = -4282.936560$  au  
     $E_{\text{gas-phase}} = -4282.956350$  au  
     $E_{\text{BSSE}} = 0.009039$  au

C	0.00000000	0.00000000	0.00000000
N	1.31295672	0.00000000	0.00000000
C	2.04675633	1.17592117	0.00000000
C	3.39627782	1.19120879	0.17743498
H	-0.51202544	0.96600354	0.10132742
H	1.47525286	2.09904591	-0.13763368
H	3.91673443	0.24470441	0.34898930
C	-0.80571845	-1.20231111	-0.06931491
C	-2.04459161	-1.25246536	0.63880725
C	-2.79073604	-2.40749171	0.65590526
C	-2.36918732	-3.57280990	-0.04459401
C	-3.11803078	-4.77583431	-0.03980191
C	-2.68564369	-5.87385204	-0.75816215
C	-1.48962448	-5.81523834	-1.51385811
C	-0.73568399	-4.66010241	-1.54340513
C	-1.15098953	-3.51835016	-0.80545656
C	-0.40142289	-2.31601400	-0.81115243
H	-2.37426070	-0.37510609	1.19657155
H	-3.72465212	-2.44522534	1.21882743
H	-4.04140479	-4.82048164	0.53956972
H	-3.26793840	-6.79532337	-0.74507233
H	-1.16165652	-6.69247934	-2.07114268
H	0.19713435	-4.60814549	-2.10633741
H	0.44010096	-2.25025497	-1.50610422
C	4.22369539	2.36701559	0.19725357
C	5.62012991	2.36482548	0.58299751
C	6.13234630	3.68459220	0.40738901
C	5.08295310	4.50787795	-0.11484609
C	3.91053046	3.70338982	-0.26003757
H	6.16172880	1.50037903	0.95604512
H	7.15241786	4.00105586	0.60269091
H	5.17184276	5.55530277	-0.38719884
H	2.95692393	4.03775781	-0.65814400
Fe	5.43137415	2.92468996	-1.35326818
C	5.51604737	1.41612978	-2.74615689

C	4.74702445	2.52340401	-3.23295474
C	5.59003874	3.68222783	-3.23769403
C	6.87762174	3.29136881	-2.74564108
C	6.82883717	1.89203614	-2.44239015
H	5.14704827	0.40707180	-2.58191592
H	3.70482330	2.48970916	-3.53587486
H	5.29892849	4.68498584	-3.53608995
H	7.73151710	3.94660546	-2.60166295
H	7.63778784	1.30068394	-2.02431070
Hg	2.40560869	-1.98861340	0.14548307
O	2.72032435	-3.52629805	1.80314963
S	3.92014367	-2.92970610	2.57575384
O	4.93377619	-3.89596805	2.99502572
O	4.34693522	-1.66462093	1.88219741
C	3.07526884	-2.31387571	4.16297880
F	3.96424060	-1.67974428	4.94705414
F	2.08744762	-1.44511707	3.83679271
F	2.54005007	-3.33953548	4.84467224
O	2.54067908	-3.47210335	-1.78476257
S	3.71247415	-2.78842503	-2.48899340
O	4.10162733	-1.56691035	-1.67646593
O	3.59737135	-2.62647415	-3.94099168
C	5.15437008	-3.99258272	-2.19660531
F	4.89401882	-5.17501581	-2.78120802
F	6.28436290	-3.48281058	-2.72118484
F	5.33037710	-4.18263737	-0.875651